PF 真空封止アンジュレータ(IVU)のインピーダンス評価:理論、シミュレーション、および測定

IMPEDANCE EVALUATION OF THE PF IN-VACUUM UNDULATOR: THEORY, SIMULATIONS, AND MEASUREMENTS

田中織雅#, A), 中村典雄 A), 帯名崇 A), 土屋公央 A), 高井良太 A), 坂中章悟 A), 山本尚人 A), 加藤龍好 A), 阿達正 A)
Olga Tanaka#, A), Norio Nakamura A), Takashi Obina A), Kimichika Tsuchiya A), Ryota Takai A), Shogo Sakanaka A), Naoto Yamamoto A), Ryukou Kato A), Masahiro Adachi A)
A) High Energy Accelerator Research Organization, KEK

Abstract

Four in-vacuum undulators (IVU) were installed to the short straight sections of the 2.5 GeV Photon Factory (PF) storage ring at KEK. The minimum gaps of IVUs are all 4 mm, therefore there is a possibility of its considerable contribution into the impedance of the entire ring. As a result, the impedance of the IVU may lead to loss of beam energy, change in bunch shape, betatron tune shift, and ultimately various beam instabilities. We evaluated the IVU longitudinal and transverse impedance using a simulation tool (CST Particle Studio) and compared the simulation results with the analytical equations and with the beam measurement results. The present work describes these results. We believe the research results could be used in the IVU design as well as could provide guidelines for design of the new components such as small aperture beam tubes which are indispensable for future light source accelerators.

INTRODUCTION

Accelerator components can interact with bunched particles through their inducing wake fields caused by impedances. Impedances lead to unwanted effects such as beam energy loss, changes in the bunch shape, betatron tune shifts, and to the various beam instabilities. Knowledge of impedances of the accelerator components is of a great importance because it allows to improve the performance the accelerator essentially. Therefore, they should be carefully estimated and evaluated in the very beginning of the design process of any high intensity machine.

At KEK Photon Factory (PF) light source, we have four newly installed in-vacuum undulators (IVUs). The IVU's vacuum chamber has a complex geometry. It consists of two taper transitions between the undulator and the beam chamber, one copper plate on the undulator magnets for RF shielding of the magnets from a beam, and two step transitions between the octagon and the taper region. Each part makes its own impact on the total frequency dependent impedance of the entire IVU. Design issues of IVU including taper regions, undulator plates and step transitions were studied (see, for example, [1-4]) and their insertion devices (IDs) were found to made small impacts on the total impedance of a machine [5]. However, the four PF IVUs has the minimum gaps of 4 mm that are much small compared to apertures of the PF normal vacuum ducts, and there is a need of the proper IVU's impedance evaluations.

To quantify IVUs induced impedance we engaged both a powerful simulation tool (Wakefield Solver of CST Particle Studio [6]), and theoretical assessments (for cross-checking the results of simulation), and, finally, an experimental reconciliation of the impedance values obtained from our studies. Such a comprehensive analysis shown in this article will be a standard procedure for the design of new accelerators. It allows to predict the thresholds of instabilities and to assess the influence of collective effects [7, 8].

A few decades ago only 2D modeling of devices with axial symmetry was available. And to evaluate the impedances of real sections of the accelerator, scientists had to rely entirely on the results of the measurements [9]. Nowadays 3D impedance simulation tools (CST Particle Studio, GdfidL, MAFIA, etc.) have comparably good reliability and improved performance. Therefore, they provide an ability to simulate IDs and accelerator components with their full geometries. For example, at PETRAIII the wakefields of the whole IVU vacuum vessel were evaluated, although it required considerable computing powers [9]. In the process of simulation of wakefields and impedances, the attention of scientists gradually shifted to the consideration of chambers with a different from circular geometries (rectangular, elliptical). Thus, we began to distinguish between dipolar (or driving) and quadrupolar (or detuning) contributions to the transverse impedance, whereas previously only talked about the impedance of the dipole mode. This new treatment gives an advantage to obtain different impedance effects on the beam dynamics. i.e. the dipolar wake provides an information about instabilities growth rate. And quadrupolar wake impacts into incoherent effects such as emittance growth and damping. This approach is a courtesy of CERN impedance group [10, 11].

This study shows how we identify the major impedance contributors and evaluate their impedance using theoretical

olga@post.kek.jp

formulas, CST Studio simulations and measurements. Now, let us discuss in details these impedance evaluations, and its experimental confirmation.

IMPEDANCE EVALUATION FOR PF IVU BY SIMULATIONS AND THEORY

PF IVU consists of three parts (see Fig. 1 a) – c)). Each of these parts impacts into the total impedance of the IVU. They are:

- Taper between the flange and the undulator (200 μm thick) for the geometrical impedance.
- Copper plate (60 μm copper and 25 μm nickel coating) on top of the undulator for the resistive-wall impedance.
- Step transition from the octagon to the rectangular chambers.

In the following each contributor will be treated separately.

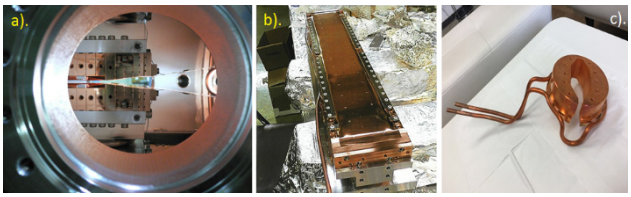

Figure 1: Three major impedance contributors of PF IVU: a) Taper between the flange and the undulator; b) Copper plate on top of the undulator; c) Step transition from the octagon to the rectangular chambers.

Geometrical Impedance of Taper

To calculate the pure geometrical impedance of the taper, we first assume the perfectly conductive material instead of using copper resistivity. The CST model of the taper is shown at Fig. 2. It is known that a very fine mesh (Δz) is needed for accurate calculations of the taper impedance. The empirical formula [12]:

$$100 \le \frac{\alpha\phi}{\Delta z}\cdot\frac{\sigma_z}{\Delta z}. \qquad (1)$$

Here α is a chamber radius, ϕ is a taper angle, and σ_z is a bunch length ($\sigma_z = 10mm$ in the case of PF ring). For PF IVU the mesh size is found to be $\Delta z \le 150\mu m$.

The IVU impedance is greatly affected by the size of its gap ($2b$ in Fig. 2). When the ID is closed, even a difference of 0.5 mm in the gap yields a drastic increase of impedance. For a better and more economical design in future, we also studied the dependence of kick factors on the taper width. Conclusion before the results are: the present 100 mm is reasonable and close to optimal width. For the future IVU designs, the length of the taper (or its angle) is one of the key parameters of impedance evaluation. Its consideration was excluded from the present study because the IVUs were already designed and installed.

The taper structure is known to produce nearly pure inductive impedance even with a vessel included.

$$Z_l = -i\omega L, \qquad W_{l0}(z) = Lc\frac{d}{dz}\delta(z/c), \qquad (2)$$

where Z_l is a longitudinal impedance of the taper, ω is a frequency, L is inductance. Theoretical formula for longitudinal impedance reads [13] (see Fig. 3, red line):

$$\frac{Z_l}{n} = -i\frac{Z_0\omega_0}{4\pi c}\int_{-\infty}^{\infty}(g')^2 F\left(\frac{g}{w}\right)dz, \qquad (3)$$

$$F(x) = \sum_{m=0}^{\infty}\frac{1}{2m+1}\mathrm{sech}^2\left((2m+1)\frac{\pi x}{2}\right)\tanh\left((2m+1)\frac{\pi x}{2}\right). \qquad (4)$$

Here Z_l/n is normalized longitudinal impedance, $Z_0 = 377\Omega$ is an impedance of the free space, ω_0 is a cyclic revolution frequency. For PF ring $\omega_0 = 2\pi\cdot 1.6MHz$. Then, g describes the vertical profile of the taper along the z axis, and w is the width of the taper.

We need a careful treatment of the transverse impedance, since it includes both the dipolar and the quadrupolar components [10]:

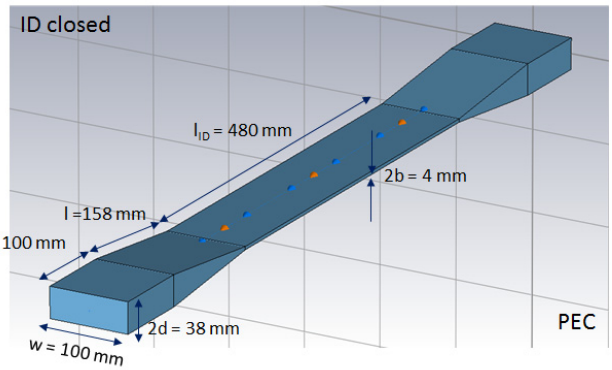

Figure 2: CST model of the IVU taper.

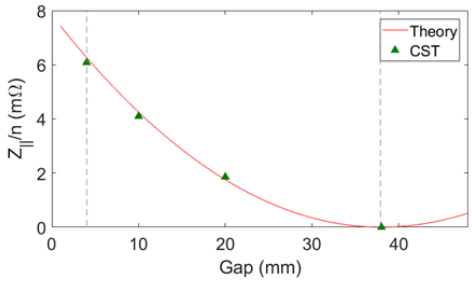

Figure 3: Normalized longitudinal impedance of the taper (gap dependence, width fixed to 100 mm) by theory (red line), and by simulations (green triangle).

$$W_{y,tot}(y_1, y_2, z) = W_{y,dip}(z)y_1 + W_{y,quad}(z)y_2, \qquad (5)$$

where $W_{y,tot}(y_1, y_2, z)$ is a total wake received by the beam. In CST simulations they can be calculated by displacing the beam and the wake integration path separately [11]. According to Krinsky [14], theoretical formula for dipolar impedance is the following:

$$Z_{yD}(k) = -i\frac{Z_0}{2\pi b}\int_{-\infty}^{\infty}\frac{\xi^2}{\sinh^2\xi}\sum_{n=0}^{\infty}\delta_n\frac{H(k_n,k)+H(k_n,-k)}{2ik_n b}d\xi \tag{6}$$

and

$$H(p,k) = \int_{-\infty}^{\infty}\int_{-\infty}^{z_1} S'(z_1)S'(z_2)e^{i(p+k)(z_1-z_2)}dz_1dz_2, \tag{7}$$

here the value k is a perturbation wave number, $k_n b = \sqrt{(kb)^2 - \xi^2 - (\pi n)^2}$, and $S(z) = (a(z) - a_0)/a_0$ denotes a fractional deviation of the taper radius from the average one (a_0). For analytical estimation of the quadrupolar impedance, a formula derived by Stupakov [13] is used:

$$Z_{yQ} = -i\frac{\pi Z_0}{4}\int_{-\infty}^{\infty}\frac{(g')^2}{g^2}G\left(\frac{g}{w}\right)dz, \tag{8}$$

with

$$G(x) = x^2\sum_{m=0}^{\infty}(2m+1) \times \operatorname{sech}^2\left((2m+1)\frac{\pi x}{2}\right)\tanh\left((2m+1)\frac{\pi x}{2}\right). \tag{9}$$

Each of dipolar and quadrupolar impedances produce vertical kick factors. In the case of Gaussian beam they relation could be expressed by the following:

$$k_y = \frac{\operatorname{Im} Z_y c}{2\sqrt{\pi}\sigma_z}. \tag{10}$$

Figs. 4 - 5 give the comparison of the analytical Eqs. (6) – (7) and (8) – (9) with the CST simulation results for the dipolar and quadrupolar vertical kicks of the taper.

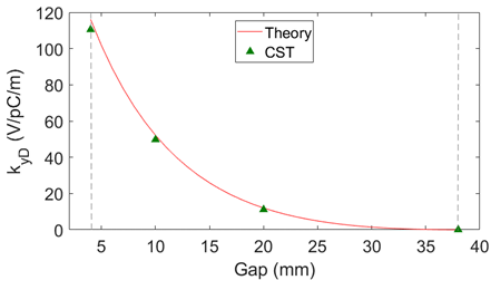

Figure 4: Dipolar vertical kick factor of the taper (gap dependence, width fixed to 100 mm) by theory (red line), and by simulations (green triangle).

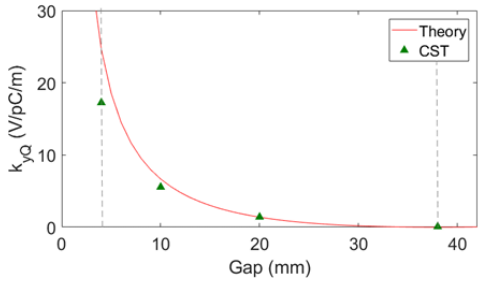

Figure 5: Quadrupolar vertical kick factor of the taper (gap dependence, width fixed to 100 mm) by theory (red line), and by simulations (green triangle).

To sum up, the calculation of kick factors is most important since it provides additional coherent vertical tune shift. During machine measurements a tune shift could be detected. It includes both of dipolar and quadrupolar impacts.

Resistive-Wall Impedance of Undulator

By using the copper resistivity in CST, we can calculate the resistive-wall impedance of the undulator with the copper plate (the electric conductivity of Cu is $\sigma_c = 5.96\times10^7\, S/m$). The vertical kick factor of the undulator plates was estimated using the following relation [15]:

$$k_{yR.W.} = \frac{cL}{8b^3}\sqrt{\frac{2Z_0 c}{\sigma_z\sigma_c}}\Gamma\left(\frac{5}{4}\right), \tag{11}$$

where L is a length of the undulator ($L = 480mm$ for PF IVU), and $\Gamma(5/4) = 0.9064$. The comparison of Eq. (11) with the CST simulation is given at Fig. 6. It demonstrates an excellent agreement between theory and simulations.

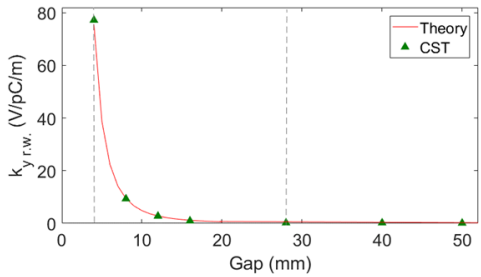

Figure 6: Resistive-wall vertical kick factor of the undulator (gap, dependence, width fixed to 100 mm, length fixed to 480 mm) by theory (red line), and by simulations (green triangle).

Geometrical Impedance of Step Transition

The impact of the step transition is three orders less than other components and thus we ignore it in the following.

Total Transverse Impedance of the IVU

The total vertical kick factor due to 1 IVU including dipolar and quadrupolar kicks of the taper and resistive-wall kick of the undulator copper plates is summarized in

Fig. 7. Table 1 provides more detailed information regarding the kick values.

An excellent agreement is seen between the theoretical predictions and the CST Studio simulations for PF IVU. Therefore, the new impedance evaluations of PF IVU are accurate enough in the framework of the theory and the simulation codes. We can use these calculation results and computation resources and techniques for future impedance measurements, for the design of a new IVUs, and even for the impedance budget of the components of any new accelerator.

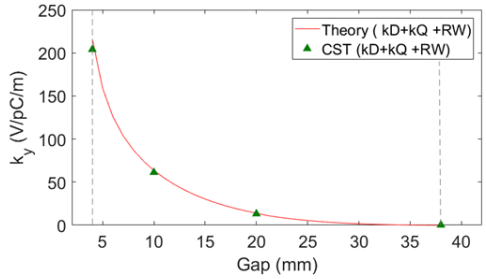

Figure 7: Total vertical kick factor of the IVU (gap dependence, width fixed to 100 mm) by theory (red line), and by simulations (green triangle).

Before moving to the next section (tune shift measurement) some preparation work should be done. Namely, we need to evaluate an additional betatron tune shift ($\Delta\nu$) by 4 IVU at PF. We are applying a well-known relation [16]:

$$\frac{\Delta\nu}{I_b} = -\frac{4\langle\beta\rangle k_y}{4\pi f_0 (E/e)}, \qquad (12)$$

where I_b is a bunch current, $f_0 = 1.6MHz$ is a revolution frequency of PF ring, and E is a beam energy (at PF $E = 2.5GeV$). With a kick data shown in Table 1, one can obtain $\Delta\nu / I_b = -9.34\times10^{-6} mA^{-1}$ as the simulation result, and $\Delta\nu / I_b = -9.98\times10^{-6} mA^{-1}$ as the analytical result. This is a reference point for our measurement.

Table 1: Vertical Kick Factors of PF IVU

Vertical kick factor per 1 IVU		CST PS	Theory
Taper vertical kick factor, V/pC/m	Dipolar	110.47	116.13
	Quadrupolar	16.64	24.61
Undulator vertical kick factor, V/pC/m	Dipolar	50.80	75.57
	Quadrupolar	26.40	
Total vertical kick factor, V/pC/m		204.31	216.31

MEASUREMENTS OF KICK FACTORS

We carried out tune shift measurements at PF based on the RF-KO (RF Knock Out) method [16]. In this method the responses of the strip line kicker oscillations were measured by sweeping the bunch current (equal to changing the betatron frequency) using a spectrum analyser equipped with a tracking generator. The switch to the single bunch operation mode and switch-off of the feedback system are crucial conditions for this measurement. In the multi-bunch mode, the current dependence of the tune shift is rather small. The feedback system introduces false signals and greatly influences the measurement result. Therefore, it is important to keep the bunch current below the instability threshold.

The additional tune shift corresponds to a difference of the vertical tune shifts for ID open (gap=38mm) and ID closed (gap=4mm) cases. We closed all four IVUs simultaneously to increase the effect. In fact, we tried to close the ID gaps one by one, and we do indicate reasonable tune shifts. The result of the tune shift measurement is shown at Fig. 8. The data were measured manually about 20 times at each current value with a step of 0.5~1 mA. We obtain the tune shift $\Delta\nu / I_b = -10.96\times10^{-6} \pm 1.86\times10^{-6}$ (including a data fitting error).

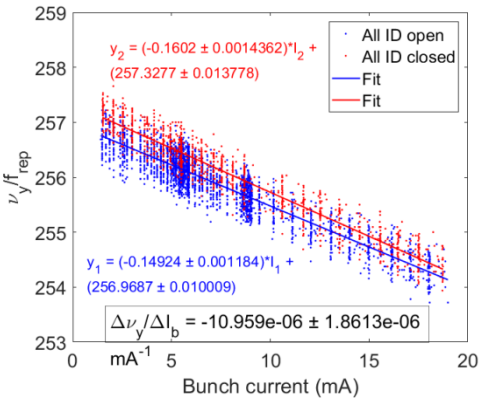

Figure 8: One of the measurement results of the additional tune shift due to the four IVU at PF.

CONCLUSION

In summary, we have identified the major impedance contributors of PF IVU and successfully evaluated their impedance using theoretical formulas, CST Studio simulations and measurements. The three evaluations show very good agreements ($\Delta\nu / I_b = -9.98\times10^{-6} mA^{-1}$ in theory; $\Delta\nu / I_b = -9.34\times10^{-6} mA^{-1}$ in simulations; and $\Delta\nu / I_b = -10.96\times10^{-6} \pm 1.86\times10^{-6}$ in the measurement). An alternative method to measure a vertical kick of the IVU, called “the orbit bump” is to create an orbit bump at the location including IVU [17-19]. We are about to implement this method for four IVUs at PF to cross-check our present kick factor evaluations. The present methods and procedures will greatly help the design of future IVU for further reduction of impedance.

ACKNOWLEDGEMENT

We would like to thank the members of PF storage ring and operational staff for their help in achieving the necessary stable injection rate to demonstrate the tune shift caused by

four IVU. Additional thanks to the monitor group for many useful advises in experimental setup.

REFERENCES

[1] V. Smaluk *et al.*, "Coupling impedance of an in-vacuum undulator: Measurement, simulation, and analytical estimation", *Phys. Rev. ST Accel. Beams*, vol. 17, p. 074402, Jul. 2014.

[2] E. Gjonaj *et al.*, "Computation of wakefields for an in-vacuum undulator at PETRA III", in *Proc., 4th Int. Particle Accelerator Conf. (IPAC 2013),* Shanghai, China, May, 2013, paper TUPWA008, pp. 1736-1738.

[3] F. Cullinan *et al.*, "Evaluation of In-Vacuum Wiggler Wakefield Impedances for SOLEIL and MAX IV", presented at the 22nd European Synchrotron Light Source Workshop (ESLS XXII), Grenoble, France, Nov. 2014; http://www.esrf.eu/files/live/sites/www/files/events/conferences/2014/XXII%20ESLS/CULLINAN_wigglerimpedance.pdf

[4] T.F. Günzel, "Coherent and incoherent tune shifts deduced from impedance modelling in the ESRF-ring", in *Proc., 9th .8.124403 European Particle Accelerator Conf. (EPAC 2004),* Lucerne, Switzerland, July, 2004, paper WEPLT083, pp. 2044-2046.

[5] T. Tanaka, "In-vacuum undulators", in *Proc., 27th Int. Free Electron Laser Conf. (FEL2005)*, Palo Alto, USA, Aug. 2005, paper TUOC001, pp. 370-377.

[6] CST-Computer Simulation Technology, CST PARTICLE STUDIO; http://www.cst.com/Content/Products/PS/Overview.aspx

[7] E. Belli *et al.*, arXiv:1609.03495.

[8] K. Bane, "Review of collective effects in low emittance rings", presented at the 2nd Topical Workshop on Instabilities, Impedance and Collective Effects (TWIICE2), Abingdon, UK, Feb. 2016; https://indico.cern.ch/event/459623/contributions/1131155/attachments/1224365/1791598/Bane_collective_ler.pdf

[9] T. Hara *et al.*, "SPring-8 in-vacuum undulator beam test at the ESRF", *Journal of Synchrotron Radiation*, vol. 5, part. 3, pp. 406-408, May. 1998.

[10] B. Salvant, "Transverse single-bunch instabilities in the CERN SPS and LHC", presented at the Beam Physics for FAIR Workshop, Bastenhaus, Germany, Jul. 2010; https://indico.gsi.de/event/1031/

[11] C. Zannini, "Electromagnetic simulation of CERN accelerator components and experimental applications", Ph.D. thesis, Phys. Dept., Ecole Polytechnique F´ed´erale de Lausanne, Lausanne, Switzerland, 2013.

[12] O. Frasciello, "Wake fields and impedances of LHC collimators", presented at the 100th National Congress of Italian Physical Society (SIF 2014), Piza, Italy, Sep. 2014.

[13] G.V. Stupakov, Phys. Rev. ST Accel. Beams 10, 094401 (2007).

[14] S. Krinsky, Phys. Rev. ST Accel. Beams 8, 124403 (2005).

[15] A. Piwinski., "Impedance in lossy elliptical vacuum chambers", DESY, Hamburg, Germany, Report No. DESY-94-068, Apr. 1994.

[16] S. Sakanaka, T. Mitsuhashi, and T. Obina, Phys. Rev. ST Accel. Beams 8, 042801 (2005).

[17] V. Kiselev and V. Smaluk, "Measurement of local impedance by an orbit bump method," Nucl. Instrum. Methods A 525, 433 (2004).

[18] L Emery, G. Decker, and J. Galayda, in *Proc., 19th Particle Accelerator Conference (PAC2001)*, Chicago, USA, Aug. 2001, paper TPPH070, pp. 1823-1825.

[19] E. Karantzoulis, V. Smaluk, and L. Tosi, Phys. Rev. ST Accel. Beams 6, 030703 (2003).